

Evidence for tip velocity oscillations in dendritic solidificationJ. C. LaCombe,^{1,*} M. B. Koss,² J. E. Frei,³ C. Giummarra,³ A. O. Lupulescu,³ and M. E. Glicksman³¹*Metallurgical and Materials Engineering, Mackay School of Mines, University of Nevada, Reno, Nevada 89436*²*Department of Physics, College of the Holy Cross, Worcester, Massachusetts 01610*³*Materials Science and Engineering Department, Rensselaer Polytechnic Institute, Troy, New York 12180*

(Received 20 July 2001; published 15 February 2002)

Dendritic growth experiments were conducted in the reduced-convection environment aboard the space shuttle Columbia on STS-87. Spectral analysis was performed on 30-frame/s video data during growths of isothermal dendrites. Results indicate that pivalic acid dendrites exhibit a subtle oscillatory behavior of the axial growth velocity near the tip, with a frequency component that is associated with the sidebranch formation process.

DOI: 10.1103/PhysRevE.65.031604

PACS number(s): 68.70.+w, 81.30.Fb, 81.70.Ha

I. INTRODUCTION

The creation of most alloy products requires that the component metals freeze from the molten state. Cast materials solidify neither all at once nor uniformly, but rather as advancing reticulated fronts that are called dendrites. These dendrites sweep through the molten phase, leaving behind a microstructure of branched crystalline morphology. It is important to understand the process by which dendrites form, because such microstructural features can persist through subsequent material processing stages and affect the properties of the finished product.

In addition to the role that dendrites play in the determination of physical properties of cast alloys, dendritic solidification constitutes a well-studied example of pattern formation in nonequilibrium physics. It is consequently a frequently discussed topic in computational condensed matter and material physics, and remains of considerable interest to physicists, mathematicians, as well as to engineers.

Despite the recognition that dendritic growth consists inherently of a coupling of steady-state propagation of the tip region and dynamic sidebranch formation behind the tip, most investigations of dendritic growth have focused on steady-state descriptions and analyses. Now, however, recognition is growing that the formation mechanism of sidebranches may be so intimately related to the tip itself that an artificial separation of the tip from the branches, enacted to make models more tractable, may actually be obscuring as much as it clarifies. Recent observations by some of the authors of this paper suggest that there may in fact not be a steady-state dendritic tip velocity. This finding drives the issues and challenges of dendritic growth towards investigations that embrace non-steady-state behavior and time-dependent dynamical considerations.

In this paper we present data and evidence for oscillatory behavior at or near the dendrite tip, observed in thermal dendrites of pure pivalic acid in the on-orbit, reduced-convection environment of the space shuttle Columbia.

II. BACKGROUND

To describe briefly the theory of dendritic growth, we follow the format used by Langer [1]. A crystalline solid, exposed to its supercooled melt, will solidify by extending the crystal-melt interface. The interface may remain relatively featureless (stable) or develop fingers, cells, or dendrites typical of instabilities that may form during growth. The motion of the freezing front is governed by the interplay between two simple and familiar processes—the irreversible diffusion of heat and the reversible work done in the formation of new surface area. In mathematical language, the shape of the emerging crystal reflects a solution of a free-boundary problem. Full mathematical descriptions of dendritic growth theories can be found in Langer's review [2], or Pelcé's book [3]. Glicksman and Marsh's review [4] provides an account of this problem that contains less mathematical detail and a more descriptive overview and references to the literature.

In practice, finding the mathematical solution to the equations describing dendritic growth proves to be difficult, if not intractable. The solution includes two elements: (1) the transport of latent heat and (2) the physics of selection, or scaling.

Over 50 years ago, Ivantsov [5] developed the first theoretical aspect, but this solution dealt only with the energy conservation and heat transfer physics. Ivantsov introduced two significant assumptions in his steady-state theory describing thermal dendrites growing in a supercooled melt: (1) that a dendrite can be represented as a shape-preserving paraboloidal interface with a tip radius R and (2) that the dendrite grows at a constant rate V . Since Ivantsov, dendrite models have been modified and expanded in several ways, each coupled to some specific "selection principle." Nonetheless, as the reviews listed above and others make clear, the speed of an advancing dendrite tip is a key characteristic of dendritic growth.

That real dendrites (as opposed to paraboloidal needle crystals) also grow in a steady-state manner, with constant velocity, is generally supported by numerous experiments on isolated dendrites (see, for example, [6,7]). Thus, most experimental and simulation studies of dendritic growth attempt to extract a constant velocity as a parametrization of

*Electronic address: lacomj@mines.unr.edu

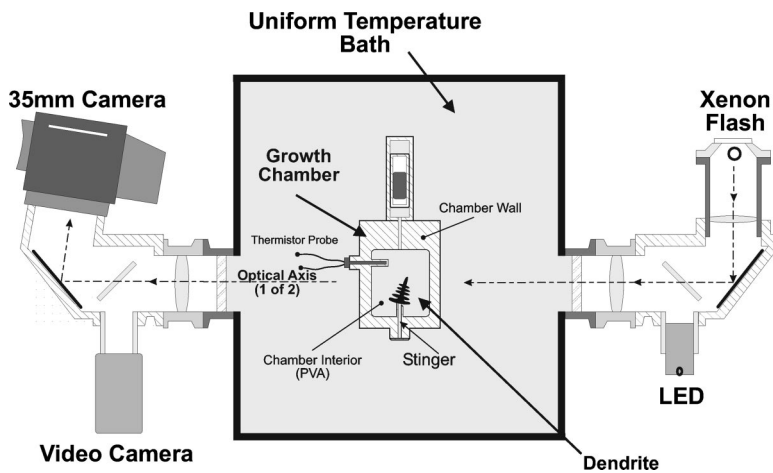


FIG. 1. Schematic representation of the experimental apparatus. Dendrites are grown within a growth chamber with four perpendicularly oriented windows, which is placed within a uniform temperature bath. After nucleation, dendrites are imaged using 30-frame/s electronic video cameras as well as 35-mm film cameras.

the kinetics; moreover, most theoretical studies also assume constant velocity behavior.

Recent work by the authors of this paper has focused on studying the thermal interactions between a dendrite and its surroundings that may explain the non-steady-state dendritic growth velocities observed [8,9]. Our analysis leads us to believe that thermal interactions between the dendrite tip and its own trailing sidebranches explains the experimental observations that growth rates do not always match predictions. Furthermore, if the strength of a dendrite's thermal interactions changes over time, the velocity of the dendrite should change as well.

Our interpretation that the sidebranch structure of a dendrite may interact with the dendrite tip and affect its growth velocity, agrees with theoretical work attempting to relate the initiation and growth of sidebranches with oscillations in the tip velocity.

The tendency of the sidebranches of a dendrite to amplify in phase with other branches pointing in directions normal to the growth axis is termed "correlation." Correlation corresponds to dendritic growth where sidebranches occur on opposite sides of the dendrite "marching in step." Such correlations are cited as evidence that the source of sidebranching instabilities is at the tip. If the tip is subject to a limit cycle, with the velocity and tip curvature oscillating in time, then these oscillations are believed to act as "coherent" perturbations that propagate in step-down each side of the dendrite. An alternative hypothesis of the source of sidebranching is that the tip is stable, propagates at steady state, and the sidebranches develop from noise. Spatial correlation of sidebranches on the dendrite, although present in some experiments, does not occur in others [10]. This suggests that the mechanism of sidebranch formation may not be universal, and, thus, sidebranches may arise from several causes.

There have been several efforts by others to measure tip oscillations during dendritic growth. These include Dougherty *et al.* [11], who studied supersaturated NH_4Br and concluded that the growth velocity lacked oscillations. Honjo *et al.* [10] reported tip oscillations in dendritic growth of NH_4Cl , constrained to thin layers. Morris and Winegard [12], also observed tip oscillations for directional solidification in the succinonitrile/camphor alloy system. All of these studies were of alloy dendrites. In alloys, which develop both

thermal and concentration fields, it is possible that periodic oscillations might arise from interactions of the thermal and solute fields, although Honjo *et al.* suggest that this mechanism cannot explain some aspects of their data. The most detailed study on dendritic tip oscillations in a pure material is by Bisang and Bilgram using xenon [13,14].

III. EXPERIMENT

A. Apparatus

The experiments described here were conducted both on earth and in the reduced-convection environment of low-earth orbit, in the payload bay of the space shuttle *Columbia* on STS-87. The apparatus is depicted schematically in Fig. 1. The pivalic acid (PVA) sample material was contained in a rigid quartz growth chamber placed in a temperature-controlled bath. The interior volume of the growth chamber was approximately 31 mm by 31 mm by 50 mm long. Nucleation of dendrites was achieved through the use of a hollow "stinger" tube that penetrated the wall of the growth chamber. The exterior end of the stinger tube was closed and capped by a thermoelectric cooler. The interior end was open, allowing the PVA sample material in the chamber to fill the stinger.

During the operation of the experiment, each growth cycle began by completely melting the sample, followed by lowering the temperature of the melt to the desired supercooling. At a desired temperature of the melt, the thermoelectric cooler was activated, nucleating a crystal in the capped end of the stinger, which then propagated down the inside wall of the stinger tube to emerge into the chamber as a freely growing dendrite. After recording images of the growth, the next growth cycle was initiated by remelting the sample and proceeding again as described above. This experimental arrangement, combined with the microgravity conditions, produced dendritic crystals grown under diffusion-limited conditions, with the bath temperature controlled to within 0.002 K (spatially and temporally). The same apparatus, post flight, was also operated on the ground to acquire an appropriate "baseline" data set describing dendritic growth under the convective conditions associated with the gravity of earth.

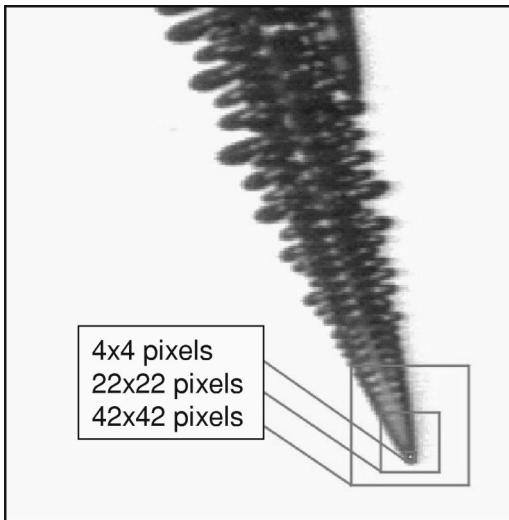


FIG. 2. Typical dendrite imaged by the electronic video camera. The supercooling was 0.397 K, the growth rate was $V = 43.7 \mu\text{m/s}$, with a vertical component of this velocity of $V_y = 41.5 \mu\text{m/s}$, and the dendrite tip radius was $R = 20.0 \mu\text{m}$ (less than one $22.3\text{-}\mu\text{m}$ -wide pixel). Three different boxes illustrate the image regions used to calculate the intensity centroid.

During the growth cycles, images of the dendrites were obtained from two perpendicular views using both electronic and film cameras. The optical system that produced the images used an f number of 40, with an illumination wavelength of 486 nm. Whereas the film images constituted the primary data source for the space shuttle/zero convection experiments, the observations described here are derived primarily from the electronic video cameras. These cameras provided both the spatial and temporal resolutions that are necessary to study the transient aspects of the growth process. Figure 2 depicts a typical dendrite tip, as imaged by the electronic video camera.

B. Data extraction

The data presented here are primarily based on measurements of dendrite tip locations as a function of the time, obtained from the 30 fps video cameras. The field of view was wide enough to include the entire dendrite growth process, and was not optimized for imaging the dendrite tip. Each pixel in the camera's 640×480 pixel array, after correcting for the magnification of the optics system, images a region of the chamber that is approximately $22 \mu\text{m}$ by $22 \mu\text{m}$, in 256 shades of gray. The pixel size sets the initial precision for the tip position data. It is necessary to improve upon the spatial precision by applying a sub-pixel-resolution image analysis method to each electronic image in the growth cycle.

Analysis of the dendrite tip's location as a function of the time began by examining the first and last image frames of a growth cycle. The dendrite tips are found in these images using a row-by-row search of the pixels, to locate the lowest pixel in the field of view that is darker than a specified threshold value. If there is more than one pixel in a row satisfying this criterion, their average is used for the horizon-

tal coordinate. With these crude estimates of the tip positions at the beginning and end of the growth, it is possible to construct a vector to predict where the tip will be during intermediate video frames throughout the growth. This tip-location scheme is capable of resolving information on the order of the pixel imaging region size of $22 \mu\text{m}$. Its main value, however, is in providing a starting point for subsequent enhancements in the tip-location measurement.

Using this first estimate of the tip location, a second stage of refinement is added to the tip-location process for each image. This is achieved by overlaying a "sampling line" along the predicted vector (i.e., the growth axis) and determining the point along this vector where the image intensity crosses a selected threshold value. The sampling line is "thick" in that it also is comprised of several pixels, creating an averaging effect. Additionally, interpolation along the vector is performed to determine the threshold location more precisely. By incorporating a statistically larger number of pixels in this second-stage tip-locating method, resolution is improved to approximately $7 \mu\text{m}$ ($\sim 1/3$ pixel).

The third and final stage of resolution enhancement is achieved by an approach that incorporates still more information related to the tip location. Using the refined tip location (stage 2, described above) as a reference location, a box is constructed around the tip of the dendrite with the box center located $1/4$ of the box size behind the tip. Figure 2 depicts such a box in three different sizes. Next, the centroid of the pixel intensity within this box is calculated. Pixels near the edges of the box are weighted to account for edge effects experienced while calculating the centroid of an object that actually extends beyond the box. In practice, the coordinates of this centroid exhibit a resolution of approximately $2 \mu\text{m}$ ($\sim 1/10$ pixel). While the Rayleigh criterion for the optical parameters reported above would predict a resolving limit of $10.5 \mu\text{m}$, this criterion is too restrictive and unrealistic because it does not account for the statistical information available through calculation of a centroid of many pixels (a form of statistical averaging). As reported earlier by the authors [8], the standard deviation of many successive tip-location measurements indicates an uncertainty of approximately $2 \mu\text{m}$ in the tip location over time.

This approach to tip-location does not locate the actual tip's interface. Instead, it uses the additional data (many more pixels) to obtain a more consistent reference point, which then serves to track the movement of the tip over time. The exact size of the sampling box used in the centroid calculation is arbitrary. Its selection provides a balance between the desire to have a large number of data points contributing to the measurement, while avoiding the inclusion of pixels from regions of the interface that are not at steady state. When the information that is obtained from regions further removed from the tip is used, nascent sidebranches could contribute to the centroid calculation.

Once extracted from the images, the tip positions are then converted into a displacement vs time data set that is used for subsequent analysis (see Fig. 3). The displacement is calculated relative to the tip position in the first available frame of video data, defined here as time=0. The measures of resolution offered herein were obtained by examining the statistical

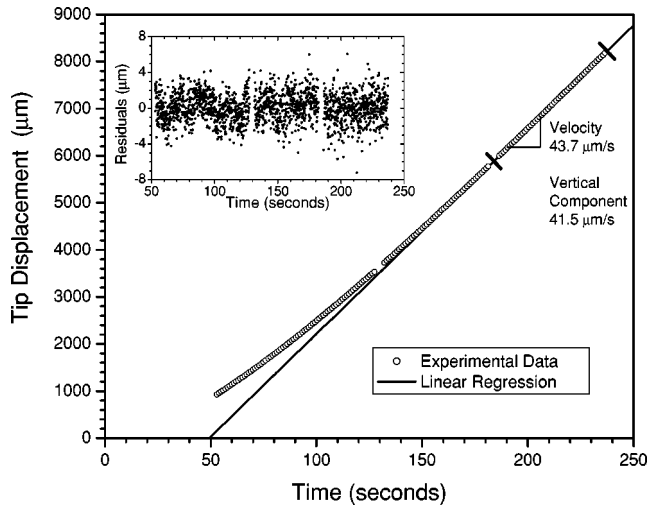


FIG. 3. Main figure: Tip displacement vs time plot for a dendrite grown at 0.397 K supercooling (1 out of every 30 data points is plotted). Data points represent the positions located via the intensity centroid. The solid line represents a first-order polynomial regression used to roughly estimate the velocity. Inset: Residuals resulting from a fourth-order polynomial fit to data in latter stage of growth. The spread in the residuals is characterized by a standard deviation of $\sim 2 \mu\text{m}$. For the inset figure, 1 of every 3 data points is plotted.

spread in the residuals produced by a linear regression of the tip displacement data.

IV. RESULTS

The results that are presented here derive from a representative growth cycle, grown at a supercooling of $\Delta T = 0.397 \text{ K}$. Qualitatively similar results have been observed in other growth cycles, but identifiable spectral peaks do not appear to be present in all growth cycles. For the data presented here, the measured steady-state growth parameters were: velocity $V = 43.7 \mu\text{m/s}$, velocity $V_y = 41.5 \mu\text{m/s}$, tip radius of curvature, $R = 20.0 \mu\text{m}$, sidebranch spacing $\lambda \approx 104 \mu\text{m}$, and the first measurable sidebranch was found approximately 45 R behind the tip.

As mentioned above, earlier observations by the authors indicated that dendritic growth rates are not constant over the time scale of observation [8]. Specifically, the dendrite tip, after completing an initial transient stage of growth, continues to experience a small acceleration. The gaps in the data of Fig. 3 resulted from the procedures used during 35-mm camera exposures. This cycle shows that after an initial transient, the dendrite evolves to a more uniform velocity (beyond $\sim 125 \text{ s}$) from which one generally extracts a “constant” velocity value. The residual acceleration of dendrites that persists late into the growth will not be discussed in detail here; for more on this issue, the reader is referred to Ref. [8]. We focus here instead on the presence of oscillatory characteristics in the tip position vs time data.

The tip displacement vs time data, obtained as described above, were evaluated to identify the possible presence of characteristic frequencies. Commonly, a discrete Fourier transform is used in this type of analysis, although that ap-

proach has inherent limitations. In order for established FFT (fast Fourier transform) algorithms to be applied, it is necessary that the data be sampled at even spacings in time. Additionally, the FFT algorithms do not accommodate gaps in the sampled data, and the more common routines operate on data sets of size equal to a power of 2. A suitable method for the spectral analysis of unevenly sampled data of arbitrary number was developed by Lomb [15]. This method is described well in [16].

Lomb’s approach produces a normalized periodogram, with spectral power as a function of the frequency. This method provides a statistical significance level that serves as a measure of the probability that a spectral peak is merely due to random noise. The spectral analysis presented here derives from the output of this Lomb periodogram method, implemented in our own code.

The effectiveness of the Lomb periodogram was confirmed through numerous test cases, where data sets were created with Gaussian noise superimposed onto multiple sinusoidal signals. The Lomb method successfully identified the correct frequencies in tests using signal amplitudes as small as 1/15 of the maximum noise amplitude. Similarly, the method was also found to be successful when applied to data sets with gaps in the data. The Lomb method is consistent with an FFT algorithm when applied to a suitable data set. Lastly, in no case did the Lomb periodogram generate false spectral peaks. Prior to applying the Lomb periodogram, the tip position vs time data were processed for better application of the spectral analysis technique. In short, the objective of the spectral analysis was to evaluate fluctuations in growth velocity. However, the growth velocity was not constant over the duration of the growth, as described in [8]; it was instead gradually accelerating throughout the period of observation. Thus, a fourth-order polynomial was least-squares fit to the displacement vs time data, and the residuals resulting from this regression were produced (see inset of Fig. 3). These residuals, i.e., the point-by-point differences between the measured dendrite tip displacement data and the smooth regressed data, were then used as the data for the spectral analysis. This is tantamount to filtering the very low frequency components of a signal.

Spectral analysis identified several statistically significant peaks in the dendrite’s displacement-time data. The peak seen at 1.87 Hz (Fig. 4) is due to the instrumentation used to image the growth process. It is an artifact of the spatial resolution of the electronic camera used in the optical system. Each pixel of the camera imaged a region of space approximately 22.3 μm in width and height, and thus a dendrite growing at a speed of $V_y = 41.5 \mu\text{m/s}$ traverses the rows of pixels at a frequency of 1.86 Hz. Figure 5 reveals that the size of some of the peaks is seen to vary with the amount of the dendrite’s tip that is used in the tip-location measurements. These data will be discussed in the following section.

V. DISCUSSION

Dendrites are stochastic in nature and are not parabolic bodies of revolution [6,17]. Since they resist quantification in

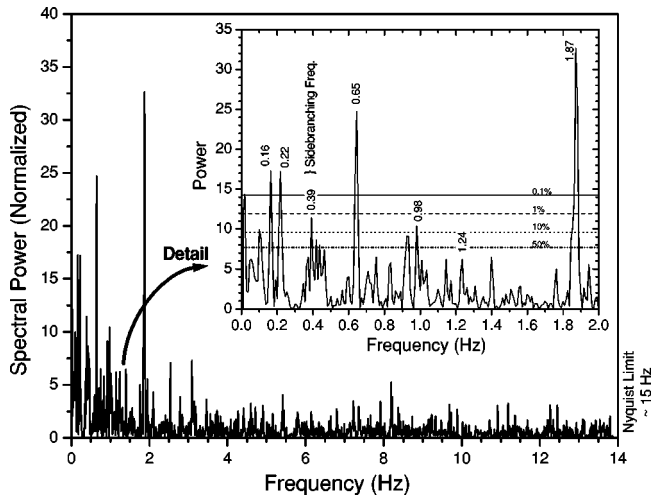


FIG. 4. Spectral components of tip displacement residuals produced by Lomb periodogram of data produced using a 22×22 pixel centroid calculation box. Inset shows details. Confidence levels (horizontal lines) represent the listed likelihood (50%–0.1%) that a peak extending to the indicated power levels is due to random influences.

anything but an “average” sense, it is conceivable that they do not grow strictly at a constant rate. For example, a “feedback” mechanism may be present in which a dendrite growing too fast, slows down, or when growing too slowly, speeds up, and naturally leads to a tip velocity oscillation. Other logical alternatives to steady-state growth include accelerating dendritic growth, or intrinsically oscillatory growth, such as a limit cycle.

The spectral band containing the 0.39 Hz peak in Fig. 4 correlates well with the frequency at which sidebranches were being created. Given a measured sidebranch spacing of $\lambda = 104 \mu\text{m}$, a dendrite growing at $V_y = 41.5 \mu\text{m/s}$ is expected to create new sidebranches at a frequency of 0.40 Hz—a frequency that agrees very well with the peaks present in the band at 0.39 Hz in Fig. 4.

These results are independent of the size of the averaging box used to locate the dendrite tip. For example, Fig. 5 demonstrates that the band at 0.39 Hz becomes more prominent as the box size increases, and data farther behind the tip (i.e., closer to the side branches) are included. Each of the three plots in Fig. 5 is produced using tip-location data derived from different sized centroid boxes. The 0.39 Hz peak’s strength increases as the centroid box size increases and extends towards the sidebranching area of the interface and is statistically significant even for the centroid calculation box of 4×4 pixels. Note, that the first visually recognizable sidebranch occurs approximately $45R$ behind the tip in PVA dendrites, which for this dendrite, corresponds to ~ 40 pixels. This location is outside of all three of the centroid calculation boxes used in producing Fig. 5. However, this figure illustrates that even in spectra derived from within $3-4R$ of the tip (4×4 pixel box), the peak associated with sidebranch formation is still present even though sidebranches become clearly apparent only ~ 13 times further behind the tip. This is evidence that the oscillation arises most likely from the tip’s axial motion, and is not likely to be caused by possible

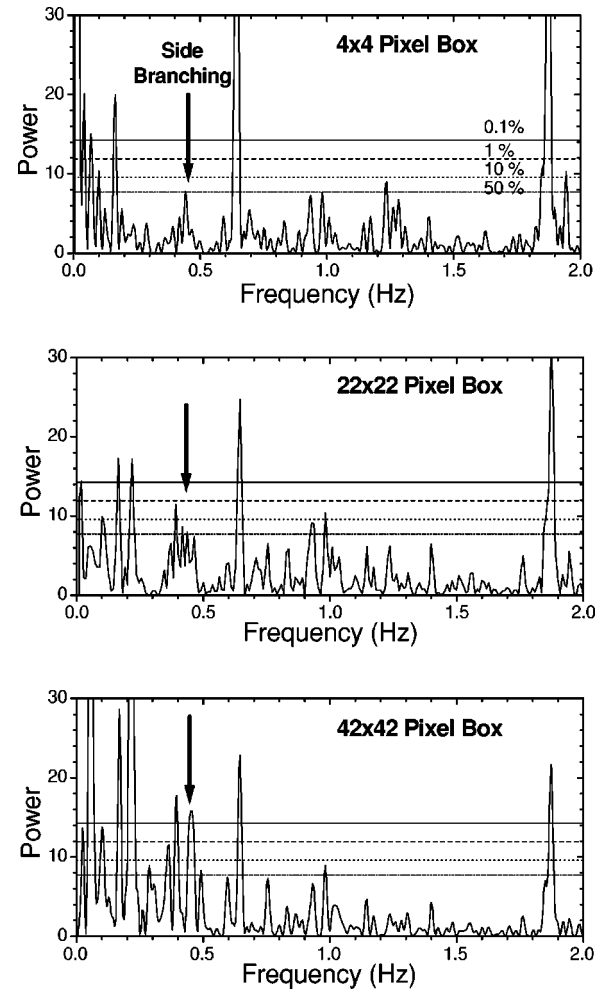


FIG. 5. Spectral plots calculated from residuals produced with three different centroid calculation box sizes. Top: 4×4 pixels, middle: 22×22 pixels, bottom: 42×42 pixels. The peaks corresponding to sidebranch formation are statistically significant in all three cases, i.e., there is less than 50% likelihood that the peaks can be explained by random influences.

tip morphology variations associated with an emerging sidebranch structure.

At present, it is not known if any of the other statistically significant peaks in the spectral power plots are representative of dendritic growth, or are due merely to experimental influences related to periodic motion in either the melt or in the mechanically mixed isothermal bath. These possibilities result from optical density gradients in these liquids due to small temperature fluctuations. These gradients are in the optical path of the light entering the video camera, and could affect the images. The convection-free environment of low-earth orbit minimizes motion in the melt. Regardless of the cause, the presence of unidentified spectral peaks needs to be acknowledged.

The spectral peaks reported here are not likely caused by thermal-solutal interactions, because the PVA test sample was highly purified ($\sim 99.99\%$). Our assessment of purity is based on the fact that the equilibrium melting temperature, which was measured several times before and during these

experiments, was $(35.902 \pm 0.002)^\circ\text{C}$. This melting point, when compared with the best known measure of the melting temperature of pure PVA, $(35.935 \pm 0.001)^\circ\text{C}$, yields the purity level as calculated by the method described by Singh and Glicksman [18].

The existence of a spectrum of tip velocity oscillation frequencies, rather than just one related to the average tip velocity and the sidebranch spacing, might confound attempts to identify tip oscillations [11,13,14]. Lastly, the amplitude of the tip velocity oscillation is smaller than the uncertainty of the assumed constant velocity dendrite. These oscillations appear to be very weak relative to signal noise, and present, in our opinion, an experimental challenge to their detection. Bisang and Bilgram reported that xenon dendrites do not show any indication of oscillations with amplitudes greater than the uncertainty, or limit of error in their measurement of the tip velocity. As expressed above, without benefit of spectral analysis on a dense data set, there may be little chance of uncovering the presence of tip oscillations. Similar comments can be made about the work of Dougherty and Gollub [19], who do not report on a tip oscillation frequency, but do report that the visible fluctuations in their velocity vs time plot are due to measurement uncertainties.

VI. SUMMARY

A method was developed for evaluating the spectral content of dendritic growth rate data. This method was applied to PVA dendrites growing in a convection-free environment.

Spectral analysis of the dendritic growth data revealed a characteristic frequency that may be intrinsic to the growth process. A peak is seen at the frequency at which sidearms are being created (0.39 Hz).

The steady-state aspects of the dendritic growth process are now reasonably well understood. However, the range of non-steady-state behaviors observed in the experiments reported here illustrates that further analysis is needed, which might reveal important information about the mechanism of dendritic growth.

ACKNOWLEDGMENTS

This work was supported by NASA under Contract Nos. NAS3-25368 and NAG8-1488. The authors wish to thank the many Rensselaer undergraduate and graduate student volunteers for assistance in operating the flight experiment aboard USMP-4. We especially thank J. J. Xu for fruitful discussions of dendritic growth theory, as well as Ken Pitolo, Tom Narita, and De-Ping Yang for discussions about the resolution capabilities. Additionally, we thank D. C. Malarik and her team at or associated with NASA's Glenn Research Center at Lewis Field for their engineering support, and the staff of the POCC/HOSC at NASA's Marshall Space Flight Center for flight operations support. Finally we thank the crew of the STS-87 for bringing our experiment to orbit and back, and for their extra efforts in providing us with quality video data for our postflight analysis.

-
- [1] J. S. Langer, in *Critical Problems in Physics*, edited by V. L. Fitch, D. R. Marlow, and M. Dementi, Princeton Series in Physics (Princeton University Press, Princeton, 1996), p. 11.
 - [2] J. S. Langer, *Rev. Mod. Phys.* **52**, 1 (1980).
 - [3] *Dynamics of Curved Fronts*, edited by P. Pelc (Academic Press, New York, 1988).
 - [4] M. E. Glicksman and S. P. Marsh, in *Handbook of Crystal Growth*, edited by D. T. J. Hurle (Elsevier Science, Amsterdam, 1993), Vol. 1, p. 1077.
 - [5] G. P. Ivantsov, *Dokl. Akad. Nauk SSSR* **58**, 567 (1947).
 - [6] S.-C. Huang and M. E. Glicksman, *Acta Metall.* **29**, 701 (1981).
 - [7] M. B. Koss, J. C. LaCombe, L. A. Tennenhouse, M. E. Glicksman, and E. A. Winsa, *Metall. Mater. Trans. A* **30A**, 3177 (1999).
 - [8] J. C. LaCombe, M. B. Koss, and M. E. Glicksman, *Phys. Rev. Lett.* **83**, 2997 (1999).
 - [9] J. C. LaCombe, M. B. Koss, D. C. Corrigan, A. O. Lupulescu, L. A. Tennenhouse, and M. E. Glicksman, *J. Cryst. Growth* **206**, 331 (1999).
 - [10] H. Honjo, S. Ohta, and Y. Sawada, *Phys. Rev. Lett.* **55**, 841 (1985).
 - [11] A. Dougherty, P. D. Kaplan, and J. P. Gollub, *Phys. Rev. Lett.* **58**, 1652 (1987).
 - [12] L. R. Morris and W. C. Winegard, *J. Cryst. Growth* **1**, 245 (1967).
 - [13] U. Bisang and J. H. Bilgram, *Phys. Rev. E* **54**, 5309 (1996).
 - [14] U. Bisang and J. H. Bilgram, *Phys. Rev. Lett.* **75**, 3898 (1995).
 - [15] N. R. Lomb, *Astrophys. Space Sci.* **39**, 447 (1976).
 - [16] W. H. Press, S. A. Teukolsky, W. T. Vetterling, and B. P. Flannery, *Numerical Recipes in FORTRAN*, 2nd ed. (Cambridge University Press, New Delhi, 1994).
 - [17] J. C. LaCombe, M. B. Koss, V. E. Fradkov, and M. E. Glicksman, *Phys. Rev. E* **52**, 2778 (1995).
 - [18] N. B. Singh and M. E. Glicksman, *Thermochim. Acta* **159**, 93 (1990).
 - [19] A. Dougherty and J. P. Gollub, *Phys. Rev. A* **38**, 3043 (1988).